

Chemistry at the Sterically Shielded Mercury Centre of the $[(\eta^4\text{-pp3})\text{PtHg}]$ Fragment

Walter Schuh,^[a] Holger Kopacka,^[a] Klaus Wurst,^[a] and Paul Peringer^{*[a]}

Keywords: Mercury / Platinum / Cluster compounds / Phosphanes / NMR spectroscopy

Treatment of $[(\eta^4\text{-pp3})\text{PtH}]\text{OTf}$ (pp3 = tris[2-(diphenylphosphanyl)ethyl]phosphane) with PhHgCl gave $[(\eta^4\text{-pp3})\text{PtHgCl}]\text{OTf}$ (**1a**) in good yield. The reaction of **1a** with the carbonylmetallates $[\text{Mn}(\text{CO})_5]^-$ or $[\text{Co}(\text{CO})_4]^-$ and TiOTf produced the linear trinuclear clusters $[(\eta^4\text{-pp3})\text{PtHgMn}(\text{CO})_5]\text{OTf}$ (**2**) or $[(\eta^4\text{-pp3})\text{PtHgCo}(\text{CO})_4]\text{OTf}$ (**3**), respectively. The reaction of **1a** with PR_3 and TiOTf gave $[(\eta^4\text{-pp3})\text{PtHg}(\text{PR}_3)](\text{OTf})_2$ (**4**: R = *n*Bu; **5**: R = Ph), with $\text{Ph}_2\text{P}(\text{CH}_2)_n\text{PPh}_2$ (*n* = 1, 2) or dppmSe [dppmSe = bis(diphenylphosphanyl)methane monoselenide] adducts in which the diphosphane/diphosphane monoselenide adopts a mono-

dentate, bridging or chelating bonding mode depending on the ligand and the stoichiometry. The mercury-bound phosphane complexes extrude elemental Hg within hours or days. The new compounds were characterised by multinuclear NMR spectroscopy and, in part, by single-crystal X-ray diffraction. The NMR investigations yielded unprecedented parameters, e.g. very large ^{31}P coordination chemical shift for a monodentate phosphane or $^2J(\text{Hg-Pt-P})$ couplings that were two to three times larger than Hg–P one-bond couplings within the same complex.

Introduction

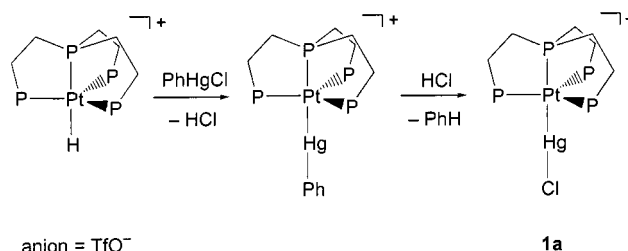
Clusters containing an unsupported mercury–platinum bond tend to extrude elemental mercury.^[1] The noticeable stability of the Pt–Hg bond in $[(\eta^4\text{-pp3})\text{PtHgPh}]\text{OTf}$ ^[2] and the closely related compound $[(\eta^4\text{-np3})\text{PtHgMe}](\text{BPh}_4)$ ^[3] (np3 = tris[2-(diphenylphosphanyl)ethyl]amine) has been attributed to the shield of the six phenyl groups of the pp3 or np3 ligand. This stimulated an investigation of the chemistry of the $[(\eta^4\text{-pp3})\text{PtHg}]$ fragment. We report here on a comfortable and high-yielding access to $[(\eta^4\text{-pp3})\text{PtHgCl}]\text{OTf}$ (**1a**), which is an appropriate compound for substitution reactions with carbonylmetallates, mono- and bidentate phosphanes, or phosphane selenides at the mercury site.

2. Results and Discussion

2.1. Syntheses and Reactions

We observed that $[(\eta^4\text{-pp3})\text{PtHgPh}]\text{OTf}$ slowly degrades in chloroform solution to give $[(\eta^4\text{-pp3})\text{PtHgCl}]\text{OTf}$ (**1a**), attributable to the presence of trace amounts of HCl in CHCl_3 , which cleave the mercury–carbon bond and leads to the substitution of the phenyl group by chloride. This was exploited in a comfortable high-yield synthesis of **1a** by treatment of $[(\eta^4\text{-pp3})\text{PtH}]\text{OTf}$ with PhHgCl according to Scheme 1: The reaction is thought to proceed by interme-

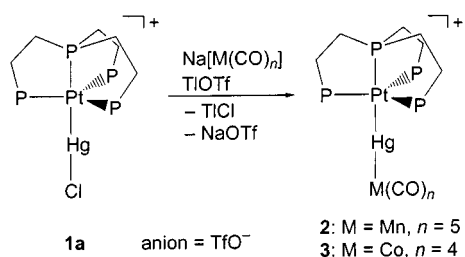
diate formation of $[(\eta^4\text{-pp3})\text{PtHgPh}]^+$, which is in turn acidolysed by HCl formed in stoichiometric amounts.



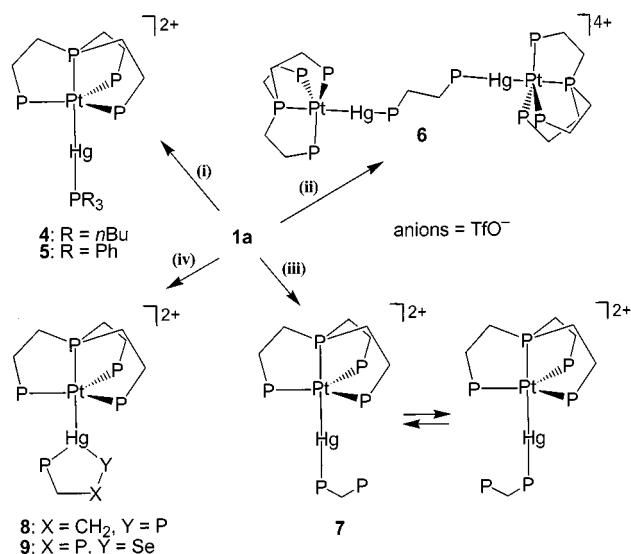
Scheme 1. Proposed synthetic pathway for **1a**

In the presence of excess chloride, **1a** slowly degrades by extrusion of elemental mercury to $[(\eta^4\text{-pp3})\text{PtCl}]\text{Cl}$.^[4] Compound **1a** is air-stable in solution and in the solid state, readily soluble in CH_2Cl_2 , slightly soluble in MeOH, and was isolated as a yellow microcrystalline powder from CH_2Cl_2 /toluene. Compound **1a** was characterised by ^{31}P , ^{195}Pt and ^{199}Hg NMR spectroscopy. Yellow crystals of $[(\eta^4\text{-pp3})\text{PtHgCl}](\text{PF}_6)\cdot\text{CH}_2\text{Cl}_2$ (**1b**· CH_2Cl_2), which were suitable for single-crystal X-ray diffraction, were obtained by slow diffusion of a methanolic solution of NH_4PF_6 into a CH_2Cl_2 solution of **1a**. The reaction of **1a** with the carbonylmetallates $[\text{Mn}(\text{CO})_5]^-$ or $[\text{Co}(\text{CO})_4]^-$ in THF and subsequent treatment with TiOTf gave the linear heterotrinuclear clusters $[(\eta^4\text{-pp3})\text{PtHgMn}(\text{CO})_5]\text{OTf}$ (**2**) and $[(\eta^4\text{-pp3})\text{PtHgCo}(\text{CO})_4]\text{OTf}$ (**3**) (Scheme 2). Both were characterised by multinuclear NMR and elemental analysis, **2** in addition by single-crystal X-ray diffraction. There are only three reports on complexes with a Pt–Hg–Mn or Pt–Hg–Co bond sequence in the literature,^[5] the compounds were characterised by spectroscopic methods, no single crystal structure determinations had been performed.

^[a] Institut für Allgemeine, Anorganische und Theoretische Chemie, Universität Innsbruck, Innrain 52a, 6020 Innsbruck, Austria
E-mail: paul.peringer@uibk.ac.at

Scheme 2. Synthesis of **2** and **3**

Treatment of **1a** with the monodentate phosphanes $PnBu_3$ and PPh_3 in the presence of TiOTf led quantitatively (according to ^{31}P NMR) to the complexes $[(\eta^4\text{-pp3})PtHg(PR_3)](OTf)_2$ (**4**: R = *n*Bu; **5**: R = Ph) as depicted in Scheme 3.

Scheme 3. (i) TiOTf/ PR_3 ; (ii) TiOTf/0.5 dppe; (iii) TiOTf/dppm; (iv) TiOTf/dppe (**8**) or TiOTf/dppmSe (**9**)

Since the complexes decompose very rapidly in the presence of halides, TiOTf was used as a chloride scavenger. In the absence of phosphanes, TiOTf is not able to abstract the chloride ligand from **1a**. This was, however, accomplished by AgOTf, but the presumptive product $[(\eta^4\text{-pp3})PtHg](OTf)_2$ immediately extruded elemental mercury. The phosphane complexes **4** and **5** decomposed within 1 d – in the presence of chloride or excess phosphane – into elemental mercury and $[(\eta^4\text{-pp3})Pt(PR_3)](OTf)_2$, which were identified according to their ^{31}P NMR spectroscopic data.^[6,7] Hence, **4** and **5** as well as the other phosphane derivatives described below could not be isolated in the solid state. The use of $P(OMe)_3$ or $P(H)Ph_2$ instead of PR_3 according to Scheme 3 immediately produced elemental mercury and the mononuclear platinum complexes $[(\eta^4\text{-pp3})Pt\{P(H)Ph_2\}](OTf)_2$ or $[(\eta^4\text{-pp3})Pt\{P(OMe)_3\}](OTf)_2$, respectively, identified by their ^{31}P NMR spectroscopic data.^[8,9]

The products of the reaction of **1a** with 0.5 equiv. of $Ph_2P(CH_2)_nPPH_2$ in the presence of TiOTf depends on *n*: Whereas dppe (*n* = 2) gives the phosphane-bridged tetra-

nuclear complex $[(\eta^4\text{-pp3})PtHg(\mu\text{-dppe})HgPt(\eta^4\text{-pp3})](OTf)_4$ (**6**) shown in Scheme 3, dppe (*n* = 1) reacts, presumably because of steric reasons, with only 0.5 equiv. of **1a** to give the complex $[(\eta^4\text{-pp3})PtHg(\eta^1\text{-dppm})](OTf)_2$ (**7**) containing monodentate dppm. Complex **7** shows a fluxional behaviour in solution, monitored by variable-temperature ^{31}P NMR spectroscopy (see below), which can be interpreted as an intramolecular end-over-end exchange between the mercury-bound and the free-dppm phosphorus atom. Compound **7** can be synthesised quantitatively (according to ^{31}P NMR spectroscopy) by treating **1a** with dppm in a molar ratio of 1:1 (Scheme 3).

The potential for mercury to increase its coordination number in the fragment $[(\eta^4\text{-pp3})PtHg]$ can be seen from the reaction of **1a** with dppe or dppmSe in a molar ratio of 1:1. As indicated in Scheme 3, we propose a chelate bonding mode of dppe and dppmSe (according to ^{31}P NMR spectroscopic results) in the complexes $[(\eta^4\text{-pp3})PtHg(\eta^2\text{-dppe})](OTf)_2$ (**8**) and $[(\eta^4\text{-pp3})PtHg(\eta^2\text{-dppmSe})](OTf)_2$ (**9**), resulting in a tricoordinate mercury centre that is part of a five-membered ring system.

2.2. NMR Spectroscopy

The NMR parameters of compounds **1–9** are collected in Tables 1 and 2. In the Tables and the subsequent discussion, the axial phosphorus atom of the platinum-bound pp3 ligand is designated as P^a , while P^e denotes the equatorial pp3 phosphorus atoms. P^3 denotes the mercury-bound phosphorus atom(s), and all other phosphorus atoms are designated as P^4 .

Table 1. NMR parameters of the compounds **1a**, **2** and **3** in CH_2Cl_2

	1a	2	3
$\delta(P^a)$	142.5	162.9	146.6
$J(P^aP^e)$	2	5	not resolved
$J(PtP^a)$	2100	1977	2032
$J(HgP^a)$	3538	2006	2692
$\delta(P^e)$	36.4	38.9	39.9
$J(PtP^e)$	2635	2889	2773
$J(HgP^e)$	412	251	299
$\delta(Pt)$	–5577	–5188	–5292
$J(HgPt)$	11010	6200	8035
$\delta(Hg)$	910	2017	1370

The one-bond Hg–Pt coupling of the linear bond sequence Pt–Hg–X is thought to give an estimate of the *trans* influence of the group X, as has been extensively exploited for linear P–Pt–X or P–Hg–X arrangements.^[10] According to Table 1 this reveals a greater *trans* influence of the $Mn(CO)_5$ fragment compared with $Co(CO)_4$, the smallest *trans* influence in the present series is exerted by the chloride ligand. One-bond Hg–Pt couplings reported in the literature range between 37610 and 2783 Hz.^[2,3,11] The size of $^1J(PtP^a)$ and $^2J(HgP^a)$ couplings of **1a–3** show a similar dependence on the ligand attached to the mercury centre. The diagonal P^a –Pt–Hg geometry effects very large two-bond Hg– P^a couplings. This is also true for compounds **4–9** (see below), and has been previously noted for

Table 2. NMR parameters of the compounds **4–9** in $\text{CH}_2\text{Cl}_2/\text{MeOH}$ (4:1)

	4 ($T = 0\text{ }^\circ\text{C}$)	5 ($T = -40\text{ }^\circ\text{C}$)	6 ($T = -60\text{ }^\circ\text{C}$)	7 ($T = -30\text{ }^\circ\text{C}$)	8 ($T = -40\text{ }^\circ\text{C}$)	9 ^[a] ($T = 20\text{ }^\circ\text{C}$)
$\delta(\text{P}^a)$	150.5	149.3	148.1	154.0	146.5	148.2
$J(\text{P}^a\text{P}^c)$	not resolved	not resolved	not resolved	not resolved	not resolved	not resolved
$J(\text{P}^a\text{P}^3)$	191	193	196	93	100	165
$J(\text{PtP}^a)$	1961	2020	2017	2010	1997	2063
$J(\text{HgP}^a)$	2726	2869	3171	2900	3362	3539
$\delta(\text{P}^c)$	36.9	41.2	38.7	41.0	36.2	36.0
$J(\text{P}^c\text{P}^3)$	10	9	9	not resolved	not resolved	6
$J(\text{PtP}^c)$	2672	2627	2650	2656	2678	2669
$J(\text{HgP}^c)$	307	343	352	294	373	364
$\delta(\text{P}^3)$	87.5	87.3	84.8	33.1	36.0	55.9
$J(\text{PtP}^3)$	577	605	604	292	279	494
$J(\text{HgP}^3)$	902	1290	1484	554	1265	1248
$J(\text{P}^3\text{P}^3')/(\text{P}^3\text{P}^4)$	—	—	64	—	—	43
$\delta(\text{P}^4)$	—	—	—	—	—	34.0

[a] **9**: $\delta(\text{Se}) = -203$, $J(\text{HgSe}) = 842$, $J(\text{SeP}^4) = 672$; $\delta(\text{Pt}) = -5526$, $\delta(\text{Hg}) = 1598$.

$[(\eta^4\text{-pp3})\text{PtHgPh}]\text{OTf}$.^[2] Even larger $^2J(\text{HgP})$ coupling constants have been observed in Hg–Ir clusters (3879–3822 Hz).^[12]

The tetranuclear complex **6** displays an $[\text{AM}_3\text{P}]_2$ spin system, the ^{199}Hg and ^{195}Pt satellites show an $\text{AA}'\text{M}_3\text{M}'_3\text{PP}'\text{X}$ pattern. This reflects the dppe-bridged structure of **6**. The values of $^1J(\text{HgP}^3)$ are 1484–902 Hz, revealing a strong *trans* influence of the $[(\eta^4\text{-pp3})\text{Pt}]$ moiety. There are only few reports on compounds exhibiting a M–Hg–P bond sequence (M = transition metal),^[11c,13] and the $^1J(\text{HgP})$ couplings in these clusters are comparatively small as well (2483–170 Hz).

Compounds **7** and **8** exhibit an AM_3P_2 spin system flanked by ^{199}Hg and ^{195}Pt satellites at temperatures given in Table 2. The bonding modes of the bidentate phosphanes dpmm and dppe in these complexes are monodentate and chelating, respectively.

The dpmm ligand in **7** is involved in an end-over-end exchange that is fast on the NMR time scale at $-30\text{ }^\circ\text{C}$. End-over-end fluxionality is also present in other mercury–dpmm complexes.^[14] The slow exchange limit is not reached at $-100\text{ }^\circ\text{C}$, the lowest temperature attained. However, significant broadening of the P^3 signal in comparison with the other ^{31}P resonances of **7** is observed at this temperature. All couplings involving P^3 as well as its chemical shift given in Table 2 may be considered as mean values of the parameters for the mercury-bound and the free-dpmm phosphorus atom. The fluxionality at $-30\text{ }^\circ\text{C}$ is responsible for the relatively small values of these parameters compared with compounds **4–6**. The preference of the monodentate bonding mode of dpmm in **7** over a chelate structure is attributed to considerable strain in four-membered Hg–dpmm rings.

The structure of **8** is based on the value of the one-bond Hg– P^3 coupling of 1265 Hz, which is comparable to the couplings observed for compounds **4–6**. No significant broadening of the P^3 signal in comparison with the other ^{31}P resonances could be observed down to $-100\text{ }^\circ\text{C}$. The relatively small values of $\delta(\text{P}^3)$, $^2J(\text{PtP}^3)$, and $^3J(\text{P}^a\text{P}^3)$ are

attributed to a nonlinear Pt–Hg– P^3 geometry as a consequence of the increased coordination number at the Hg atom. This is in keeping with the data of **9**.

Compound **9** involving the potentially bidentate ligand dpmmSe shows an AM_3PX spin system in the $^{31}\text{P}\{^1\text{H}\}$ NMR spectrum flanked by ^{199}Hg , ^{195}Pt , and ^{77}Se satellites. The value for Hg– P^3 coupling approximately coincides with that found for **8**, revealing an Hg– P^3 bond. The coordination of the selenium atom to the mercury centre is inferred by an Hg–Se coupling of 842 Hz compared with a range for $^1J(\text{HgSe})$ couplings of 960–750 Hz.^[15] The reduced value of $^1J(\text{SeP}^4)$ with respect to the free ligand is also indicative for the coordination of Se.^[15] Due to the value of $^2J(\text{PtP}^3)$ (494 Hz) ranging between that found in **6**, with an essentially linear Pt–Hg–P geometry, and **8**, with a symmetrically bent Pt–Hg–P arrangement, we suppose an asymmetric coordination geometry around the Hg atom in **9**, where P^3 is shifted towards the Pt–Hg vector and Se is consequently shifted away. The magnitude of $^3J(\text{P}^a\text{P}^3)$ (165 Hz) is in agreement with this presumption. A related angular dependence for two-bond P–Hg–P coupling constants has been pointed out by Dakternieks.^[16] The asymmetric bonding of P^3 and Se in **9** is thought to be caused by steric demands.

The most exciting feature of compounds **4–6**, **8**, and **9** is that the Hg– P^a coupling constants over two bonds are larger by a factor of two to three than the corresponding $^1J(\text{HgP}^3)$ couplings within the same molecule (compound **7** has not been considered in this context, because Hg–P one-bond couplings are not accessible due to chemical exchange). This observation implies that care should be taken for the assignment of connectivities in mercury-containing clusters on the basis of the magnitudes of Hg–P coupling constants.

Complexes **4–6**, for which an essentially linear Pt–Hg– P^3 arrangement is anticipated, are characterised by very large ^{31}P shifts of the mercury-coordinated phosphorus atom. The corresponding coordination shifts ($\Delta\delta$) amount up to +120 ppm in compound **4**. Slightly lower

values were found for the mercury-bound phosphanes in the compounds $[\text{L}'\text{HgMo}(\text{CO})_2\text{L}(\eta^5\text{-C}_5\text{H}_5)](\text{BF}_4)$ ($\text{L}' = \text{PPh}_3, \text{PCy}_3$; $\text{L} = \text{CO}$, diverse phosphane ligands),^[13a] where the mercury atom is dicoordinated by Mo and P.

2.3. Crystallography

Yellow crystals of $[(\eta^4\text{-pp3})\text{PtHgCl}](\text{PF}_6) \cdot \text{CH}_2\text{Cl}_2$ (**1b**· CH_2Cl_2) were grown by slow diffusion of a methanolic solution of NH_4PF_6 into a CH_2Cl_2 solution of $[(\eta^4\text{-pp3})\text{PtHgCl}]\text{OTf}$. The molecular structure of the complex cation of **1b** is shown in Figure 1, selected bond lengths and angles are collected in Table 3.

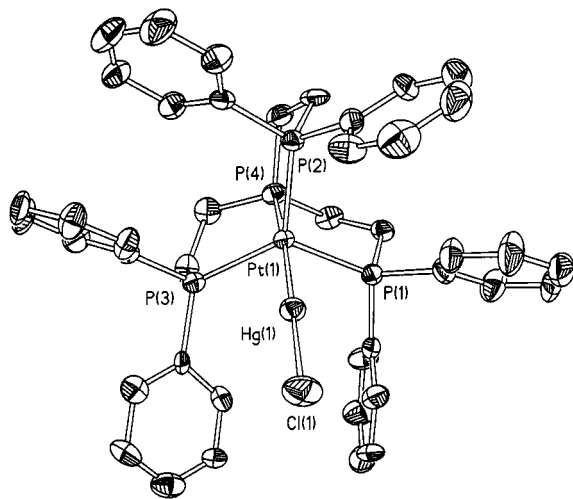


Figure 1. Molecular structure of the complex cation of **1b**· CH_2Cl_2

Table 3. Selected bond lengths [pm] and angles [°] in **1b**· CH_2Cl_2

Hg(1)–Cl(1)	237.7(2)	Cl(1)–Hg(1)–Pt(1)	174.63(7)
Hg(1)–Pt(1)	255.11(9)	P(4)–Pt(1)–Hg(1)	172.96(6)
Pt(1)–P(4)	224.3(2)	P(3)–Pt(1)–Hg(1)	89.11(6)
Pt(1)–P(3)	230.9(2)	P(1)–Pt(1)–Hg(1)	90.80(6)
Pt(1)–P(1)	233.4(2)	P(2)–Pt(1)–Hg(1)	100.98(6)
Pt(1)–P(2)	235.1(2)		

The platinum atom of the complex cation of **1b** exhibits a quasi-trigonal-bipyramidal coordination sphere with the central pp3 phosphorus atom and the mercury centre in axial positions and the three terminal pp3 phosphorus ligands in equatorial positions. The mercury atom is dicoordinated by Pt and Cl in an approximately linear manner. The Pt–Hg distance is very similar to that found in $[(\eta^4\text{-np3})\text{PtHgMe}](\text{BPh}_4)$ (253.1 pm),^[3] the Hg–Cl bond length is slightly increased compared to that in HgCl_2 (225 pm).^[17]

The Pt–Hg–Cl angle amounts to $174.63(7)^\circ$ in keeping with the absence of any $\text{Hg}\cdots\text{Cl}$ interactions with chloride ions of other cations. This is most likely the result of the steric shielding of the phenyl groups of the pp3 ligand and/or the poor acceptor qualities of the mercury centre.

Yellow crystals of $[(\eta^4\text{-pp3})\text{PtHgMn}(\text{CO})_5]\text{OTf} \cdot 1.5 \text{CH}_2\text{Cl}_2$ (**2**·1.5 CH_2Cl_2) were obtained at -19°C from a solution of **2** in $\text{MeOH}/\text{CH}_2\text{Cl}_2$ (1:1) saturated at room temperature. The crystals contain two crystallographically inde-

pendent $[(\eta^4\text{-pp3})\text{PtHgMn}(\text{CO})_5]\text{OTf}$ entities per asymmetric unit both possessing very similar geometries. The molecular structure of one of the crystallographically independent complex cations of **2** is shown in Figure 2, selected bond lengths and angles are collected in Table 4.

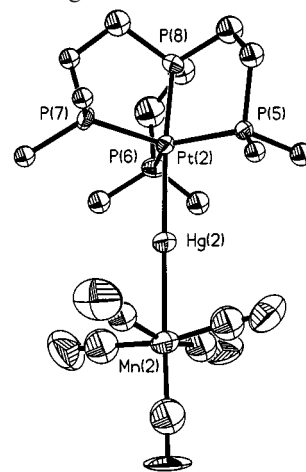


Figure 2. Molecular structure of one of the crystallographically independent complex cations in **2**·1.5 CH_2Cl_2 ; for clarity only the *ipso*-carbon atoms of the phenyl groups attached to the pp3 phosphorus atoms are shown

Table 4. Selected bond lengths [pm] and angles [°] in **2**·1.5 CH_2Cl_2

Hg(1)–Pt(1)	260.5(2)	P(3)–Pt(1)–Hg(1)	95.0(2)
Hg(1)–Mn(1)	264.7(5)	P(1)–Pt(1)–Hg(1)	93.1(2)
Hg(2)–Pt(2)	259.0(2)	P(8)–Pt(2)–Hg(2)	175.1(2)
Hg(2)–Mn(2)	261.8(4)	P(6)–Pt(2)–Hg(2)	93.5(2)
Pt(1)–P(4)	223.6(7)	P(5)–Pt(2)–Hg(2)	89.1(2)
Pt(1)–P(2)	231.5(7)	P(7)–Pt(2)–Hg(2)	97.3(2)
Pt(1)–P(3)	233.3(7)	C(4)–Mn(1)–Hg(1)	84(2)
Pt(1)–P(1)	233.5(7)	C(1)–Mn(1)–Hg(1)	84.4(13)
Pt(2)–P(8)	224.4(7)	C(5)–Mn(1)–Hg(1)	176.4(11)
Pt(2)–P(6)	229.7(7)	C(2)–Mn(1)–Hg(1)	83.7(13)
Pt(2)–P(5)	230.5(7)	C(3)–Mn(1)–Hg(1)	84(2)
Pt(2)–P(7)	232.5(6)	C(7)–Mn(2)–Hg(2)	79.5(10)
Pt(1)–Hg(1)–Mn(1)	178.96(14)	C(8)–Mn(2)–Hg(2)	84.4(11)
Pt(2)–Hg(2)–Mn(2)	176.12(12)	C(9)–Mn(2)–Hg(2)	82.7(9)
P(4)–Pt(1)–Hg(1)	177.7(2)	C(10)–Mn(2)–Hg(2)	178.2(11)
P(2)–Pt(1)–Hg(1)	91.7(2)	C(6)–Mn(2)–Hg(2)	84.4(11)

The platinum atom of the complex cation of **2** exhibits a quasi-trigonal-bipyramidal coordination sphere, with the central pp3 phosphorus atom and Hg in axial positions and the three terminal pp3 phosphorus ligands in equatorial positions. The mercury atom is dicoordinated by Pt and Mn in an approximately linear manner, Mn showing a slightly distorted octahedral environment. The Pt–Hg distances are slightly longer than in **1b**, the Hg–Mn bond lengths are increased in comparison with the compounds $[\{\eta^2\text{-(2-ClC}_6\text{H}_4)_2\text{N}_3\}\text{HgMn}(\text{CO})_5]$ (255.7 pm)^[18] and $[\text{Hg}\{\text{Mn}(\text{CO})_5\}_2]$ (260.8, 261.0 pm).^[19]

Experimental Section

Elemental analyses were performed by the Institut für Physikalische Chemie, Universität Wien. – $^3\text{P}\{^1\text{H}\}$ NMR spectra were re-

corded at variable temperatures (if not otherwise stated at 20 °C) with a Bruker DPX 300 spectrometer, and were referenced against external 85% H_3PO_4 . $^{199}\text{Hg}\{^1\text{H}\}$, $^{195}\text{Pt}\{^1\text{H}\}$, and $^{77}\text{Se}\{^1\text{H}\}$ NMR spectra were recorded at 20 °C with the same instrument and referenced against external 2 mmol HgO in 1 mL of 60% HClO_4 , 1 mol/1 Na_2PtCl_6 and neat SeMe_2 , respectively. Compound $[(\eta^4\text{-pp3})\text{PtCl}]\text{Cl}^{[4]}$ and solutions of $\text{Na}[\text{Mn}(\text{CO})_5]$ and $\text{Na}[\text{Co}(\text{CO})_4]$ in THF^[20] were prepared according to literature procedures, all other compounds were purchased from commercial suppliers and used without further purification. If not stated otherwise, all reactions were carried out under an inert gas in absolute solvents purified by standard procedures.

$[(\eta^4\text{-pp3})\text{PtHgCl}]\text{OTf}$ (1a**):** A suspension of $[(\eta^4\text{-pp3})\text{PtCl}]\text{Cl}$ (936.7 mg, 1 mmol) in $\text{CH}_2\text{Cl}_2/\text{MeOH}$ 4:1 (25 mL) was treated with NaBH_4 (113.4 mg, 3 mmol), which was added under vigorous stirring in small portions over a period of 10 min. The resulting pale yellow solution was stirred for 1 h. The organic phase was washed four times with water (10 mL). This represents a slightly modified synthesis of $[(\eta^4\text{-pp3})\text{PtH}]\text{Cl}$ to that reported by Brüggeller.^[21] $[(\eta^4\text{-pp3})\text{PtH}]\text{Cl}$ was then treated with a solution of TiOTf (353.4 mg, 1 mmol) in MeOH (2 mL), and $[(\eta^4\text{-pp3})\text{PtH}]\text{OTf}$ formed by anion metathesis and precipitation of TiCl . The precipitate was separated by centrifugation, the pale yellow solution was concentrated to dryness in vacuo. The residue was redissolved in 20 mL of CH_2Cl_2 , then treated with PhHgCl (313.2 mg, 1 mmol) and stirred for 24 h. After filtration, the clear yellow solution was concentrated to a volume of ca. 2 mL, then $[(\eta^4\text{-pp3})\text{PtHgCl}]\text{OTf}$ (**1a**) was precipitated by addition of toluene (20 mL). The product was separated by centrifugation and dried in vacuo. Yield: 1.08 g (89%).

$[(\eta^4\text{-pp3})\text{PtHgCl}](\text{PF}_6)\cdot\text{CH}_2\text{Cl}_2$ (1b**):** Yellow crystals were grown by slow diffusion of a methanolic solution of NH_4PF_6 into a CH_2Cl_2 solution of $[(\eta^4\text{-pp3})\text{PtHgCl}]\text{OTf}$. – $\text{C}_{43}\text{H}_{42}\text{ClF}_6\text{HgP}_5\text{Pt}\cdot\text{CH}_2\text{Cl}_2$ (1258.8): calcd. C 39.33, H 3.30; found C 39.05, H 3.25.

$[(\eta^4\text{-pp3})\text{PtHgMn}(\text{CO})_5]\text{OTf}$ (2**):** A solution of $\text{Na}[\text{Mn}(\text{CO})_5]$ (0.05 mmol) in THF (0.25 mL) was added to **1a** (62.5 mg, 0.05 mmol) and stirred for 5 min. After evaporation of the solvent, the residue was redissolved in CH_2Cl_2 (0.5 mL) and treated with a solution of TiOTf (17.7 mg, 0.05 mmol) in MeOH (0.2 mL). The resulting precipitate of TiCl was removed by centrifugation and the clear orange solution was concentrated until precipitation of $[(\eta^4\text{-pp3})\text{PtHgMn}(\text{CO})_5]\text{OTf}$ (**2**) began. A small amount of CH_2Cl_2 was added to redissolve the precipitate and the solution left for crystallisation at -19°C for 2 d. Yield: 30 mg (43%). – $\text{C}_{48}\text{H}_{42}\text{F}_3\text{HgMnO}_8\text{P}_4\text{PtS}$ (1410.4): calcd. C 40.88, H 3.00; found C 40.47, H 2.87.

$[(\eta^4\text{-pp3})\text{PtHgCo}(\text{CO})_4]\text{OTf}$ (3**):** A solution of $\text{Na}[\text{Co}(\text{CO})_4]$ (0.05 mmol) in THF (0.25 mL) was added to **1a** (62.5 mg, 0.05 mmol) and stirred for 5 min. After evaporation of the solvent, the residue was redissolved in CH_2Cl_2 (0.5 mL) and treated with a solution of TiOTf (17.7 mg, 0.05 mmol) in MeOH (0.2 mL). The resulting precipitate of TiCl was removed by centrifugation and the clear yellow solution washed two times with 1 mL of water. The solvent was then evaporated, the residue dissolved in CH_2Cl_2 (0.2 mL) and the product precipitated by addition of petroleum ether ($60\text{--}70^\circ\text{C}$) (2 mL). The yellow precipitate was collected by centrifugation and dried in vacuo. Yield: 52 mg (76%). – $\text{C}_{47}\text{H}_{42}\text{CoF}_3\text{HgO}_7\text{P}_4\text{PtS}$ (1386.4): calcd. C 40.72, H 3.05; found C 40.78, H 2.95.

Table 5. Crystal data and structure refinement for **1b**· CH_2Cl_2 and **2**· $1.5\text{CH}_2\text{Cl}_2$.

	1b · CH_2Cl_2	2 · $1.5\text{CH}_2\text{Cl}_2$
Empirical formula	$\text{C}_{42}\text{H}_{42}\text{ClF}_6\text{HgP}_5\text{Pt}\cdot\text{CH}_2\text{Cl}_2$	$\text{C}_{48}\text{H}_{42}\text{F}_3\text{HgMnO}_8\text{P}_4\text{PtS}\cdot 1.5\text{CH}_2\text{Cl}_2$
Molecular mass	1331.66	1537.76
Crystal system	monoclinic	monoclinic
Space group	$P2_1/n$ (no. 14)	$P2_1/c$ (no. 14)
Unit cell dimensions	$a = 1928.8(3)$ pm $b = 1406.8(2)$ pm, $\beta = 119.00(2)^\circ$ $c = 1950.5(4)$ pm	$a = 1943.7(4)$ pm $b = 3220.1(6)$ pm, $\beta = 94.44(2)^\circ$ $c = 1741.1(4)$ pm
Volume	$4.6290(14)$ nm ³	$10.865(4)$ nm ³
Z	4	8
Temperature	213(2) K	218(2) K
Density (calculated)	1.911 Mg/m ³	1.880 Mg/m ³
Absorption coefficient	6.733 mm ⁻¹	5.982 mm ⁻¹
$F(000)$	2560	5944
Color, Habit	yellow prism	yellow prism
Crystal size	$0.65 \times 0.35 \times 0.35$ mm	$0.5 \times 0.3 \times 0.25$ mm
θ range for data collection	$2.53\text{--}23.00^\circ$	$2.07\text{--}19.50^\circ$
Index ranges	$0 < h < 19$, $0 < k < 15$, $-20 < l < 19$	$-18 < h < 18$, $-30 < k < 0$, $0 < l < 14$
Reflections collected	6076	8512
Independent reflections	5860 ($R_{\text{int}} = 0.0341$)	8465 ($R_{\text{int}} = 0.0645$)
Reflections with $I > 2\sigma(I)$	4815	5162
Max./min. transmission	1.000/0.710	0.876/0.575
Data/restraints/parameters	5598/0/532	7260/0/793
Goodness-of-fit on F^2	1.064	1.038
Final R indices [$I > 2\sigma(I)$]	$R1 = 0.0344$, $wR2 = 0.0757$	$R1 = 0.0613$, $wR2 = 0.1176$
R indices (all data)	$R1 = 0.0507$, $wR2 = 0.0822$	$R1 = 0.1372$, $wR2 = 0.2731$
Largest diff. peak/hole	$764/-1057$ e ⁻ nm ⁻³	$1004/866$ e ⁻ nm ⁻³
Scan speed	variable; $7.0\text{--}35.0^\circ/\text{min}$ in ω	variable; $7.0\text{--}35.0^\circ/\text{min}$ in ω
Scan range (ω)	0.8°	0.75°
Weighting scheme	calcd. $w = 1/[\sigma^2(F_o^2) + (0.0417\cdot P)^2 + 7.0681\cdot P]$, where $P = (F_o^2 + 2\cdot F_c^2)/3$	calcd. $w = 1/[\sigma^2(F_o^2) + (0.0437\cdot P)^2 + 175.1567\cdot P]$, where $P = (F_o^2 + 2\cdot F_c^2)/3$

$[(\eta^4\text{-pp3})\text{PtHg}(\text{L})](\text{OTf})_2$ (**4**: $\text{L} = \text{PnBu}_3$; **5**: $\text{L} = \text{PPh}_3$; **7**: $\text{L} = \text{dppm}$; **8**: $\text{L} = \text{dppe}$; **9**: $\text{L} = \text{dppmSe}$): TiOTf (17.7 mg, 0.05 mmol) was dissolved in MeOH (0.1 mL) and **1a** (62.5 mg, 0.05 mmol) added with stirring to give a yellow suspension. The ligand (0.05 mmol) and CH_2Cl_2 (0.4 mL) were added and the suspension stirred for 5 min. After this, the precipitate of TiCl was separated from the yellow solution by centrifugation. All compounds rapidly decompose by extrusion of elemental mercury and could not be obtained analytically pure in the solid state.

$[(\eta^4\text{-pp3})\text{PtHg}(\mu\text{-dppe})\text{HgPt}(\eta^4\text{-pp3})](\text{OTf})_4$ (**6**): TiOTf (17.7 mg, 0.05 mmol) was dissolved in MeOH (0.1 mL) and **1a** (62.5 mg, 0.05 mmol) added with stirring to give a yellow suspension. The ligand (0.05 mmol) and CH_2Cl_2 (0.4 mL) were added and the suspension stirred for 5 min. After this, the precipitate of TiCl was separated from the yellow solution by centrifugation. Compound **6** rapidly decomposed by extrusion of elemental mercury and could not be obtained analytically pure in the solid state.

X-ray Structure Determinations: Crystals of **1b**· CH_2Cl_2 and **2**· $1.5\text{CH}_2\text{Cl}_2$ were examined by similar procedures. Crystals were mounted on a glass fibre, X-ray data were collected with a Siemens P4 diffractometer using Mo- K_α radiation ($\lambda = 71.073$ pm, monochromator: highly oriented graphite crystal, ω scan). Unit cell parameters were determined from 30–41 randomly selected reflections in the range $\theta = 5.3\text{--}12.5^\circ$, obtained by P4 automatic routine. Every 97 reflections 3 standard reflections were measured. Data were corrected for Lorentz polarisation and absorption effects (ψ scans). The structures were solved by direct methods and subsequent difference Fourier techniques (SHELXS-86).^[22] Refinement on F^2 was carried out by full-matrix least-squares techniques (SHELXL-93).^[23] All non-hydrogen atoms in the structure of **1b** as well as all non-hydrogen and non-carbon atoms in the structure of **2** were refined anisotropically, the carbon atoms in structure of **2** were refined isotropically. All hydrogen atoms were placed at calculated ideal positions (riding model). Crystal data and details of structure determinations and refinements are collected in Table 5. Crystallographic data (excluding structure factors) for the structure of **1b**· CH_2Cl_2 and **2**· $1.5\text{CH}_2\text{Cl}_2$ have been deposited with the Cambridge Crystallographic Data Centre as supplementary publication numbers CCDC-157011 and -157010. Copies of the data can be obtained free of charge on application to CCDC, 12 Union Road, Cambridge CB21EZ, UK [Fax: (internat.) + 44-1223/336-033; E-mail: deposit@ccdc.cam.ac.uk].

Acknowledgments

Financial support by the Jubiläumsfonds der Österreichischen Nationalbank (Proj.-Nr. 7416) is gratefully acknowledged.

[1] [1a] V. I. Sokolov, O. A. Reutov, *Coord. Chem. Rev.* **1978**, 27, 89. — [1b] V. I. Sokolov, V. V. Bashilov, O. A. Reutov, *J. Organomet. Chem.* **1975**, 97, 299.

[2] A. Handler, P. Peringer, E. P. Müller, *J. Organomet. Chem.* **1990**, 389, C23.

- [3] C. A. Ghilardi, S. Midollini, S. Moneti, A. Orlandini, G. Scapacci, D. Dakternieks, *J. Chem. Soc., Chem. Commun.* **1989**, 1686.
- [4] R. B. King, R. N. Kapoor, M. S. Saran, P. N. Kapoor, *Inorg. Chem.* **1971**, 10, 1851.
- [5] [5a] O. Rossell, M. Seco, G. Segales, S. Alvarez, *Organometallics* **1994**, 13, 2205. — [5b] R. A. T. Gould, L. H. Pignolet, *Inorg. Chem.* **1994**, 33, 40. — [5c] O. Rossell, M. Seco, I. Torra, *J. Chem. Soc., Dalton Trans.* **1986**, 1011.
- [6] J. Schwald, *Thesis*, University of Innsbruck, **1989**, p. 61.
- [7] M. Peter, P. Peringer, E. P. Müller, *J. Chem. Soc., Dalton Trans.* **1991**, 2459.
- [8] A. Handler, P. Peringer, E. P. Müller, *J. Chem. Soc., Dalton Trans.* **1990**, 3725.
- [9] P. Brüggeller, *Inorg. Chem.* **1987**, 26, 4125.
- [10] T. G. Appleton, H. C. Clark, L. E. Manzer, *Coord. Chem. Rev.* **1973**, 10, 335.
- [11] [11a] M. C. Janzen, M. C. Jennings, R. J. Puddephatt, *Inorg. Chem.* **2001**, 40, 1728. — [11b] L. Hao, J. Vittal, R. J. Puddephatt, *Organometallics* **1996**, 15, 3115. — [11c] K.-H. Dahmen, D. Imhof, L. M. Venanzi, T. Gerfin, V. Gramlich, *J. Organomet. Chem.* **1995**, 486, 37. — [11d] P. Braunstein, M. Knorr, M. Strampfer, A. Tiripicchio, F. Ugozzoli, *Organometallics* **1994**, 13, 3038. — [11e] M. Krumm, E. Zangrando, L. Randaccio, S. Menzer, A. Danzmann, D. Holtherrich, B. Lippert, *Inorg. Chem.* **1993**, 32, 2183. — [11f] A. Albinati, K.-H. Dahmen, F. Demartin, J. M. Forward, C. J. Longley, D. M. P. Mingos, L. M. Venanzi, *Inorg. Chem.* **1992**, 31, 2223. — [11g] Y. K. Grishin, V. A. Roznyatovskii, Y. A. Ustynyuk, S. N. Titova, G. A. Domrachev, G. A. Razuvaev, *Polyhedron* **1983**, 2, 895.
- [12] [12a] A. L. Balch, V. J. Catalano, *Inorg. Chem.* **1992**, 31, 2730. — [12b] P. I. van Vliet, J. Kuyper, D. Vrieze, *J. Organomet. Chem.* **1976**, 122, 99.
- [13] [13a] D. F. Mullica, S. L. Gipson, L. C. Snell, E. L. Sappenfield, D. H. Leschnitzer, *Polyhedron* **1992**, 11, 2265. — [13b] P. Braunstein, L. Douce, M. Knorr, M. Strampfer, M. Lanfranchi, A. Tiripicchio, *J. Chem. Soc., Dalton Trans.* **1992**, 331. — [13c] M. Cano, J. A. Campo, *Polyhedron* **1991**, 10, 2611. — [13d] A. Knoepfner-Mühlecker, W. Schuh, B. Scheffter, H. Kopacka, K. Wurst, P. Peringer, *Inorg. Chim. Acta* **2000**, 303, 70.
- [14] [14a] P. Peringer, M. Lusser, *Inorg. Chem.* **1985**, 24, 109. — [14b] P. A. W. Dean, R. S. Srivastava, *Can. J. Chem.* **1985**, 63, 2829.
- [15] [15a] A. M. Bond, R. Colton, J. Ebner, *Inorg. Chem.* **1988**, 27, 1697. — [15b] I. J. Colquhoun, W. McFarlane, *J. Chem. Soc., Dalton Trans.* **1981**, 658.
- [16] D. Dakternieks, *Inorg. Chim. Acta* **1984**, 89, 209.
- [17] [17a] H. Braekben, W. Scholten, *Z. Kristallogr.* **1934**, 89, 448. — [17b] D. Grdenic, *Arkiv. Kemi.* **1950**, 22, 14.
- [18] P. E. Jaitner, P. Peringer, G. Huttner, L. Zsolnai, *Transition Met. Chem.* **1981**, 6, 86.
- [19] [19a] M. L. Katcher, G. L. Simon, *Inorg. Chem.* **1972**, 11, 1651. — [19b] W. Clegg, P. J. Wheatly, *J. Chem. Soc. A* **1971**, 3572.
- [20] J. K. Ruff, W. J. Schlientz, *Inorg. Synth.* **1974**, 15, 84.
- [21] P. Brüggeller, *Inorg. Chim. Acta* **1987**, 129, L27.
- [22] G. M. Sheldrick, *SHELXS-86, Program for crystal structure solutions*, Göttingen, **1986**.
- [23] G. M. Sheldrick, *SHELXL-93, Program for refinement of crystal structures*, Göttingen, **1993**.

Received February 18, 2001

[101061]